Detection of Intestinal Tumors Outside the Visibility of Capsule Endoscopy Camera Utilizing Radio Signal Recognition

Mariella Särestöniemi[1,2(✉)], Attaphongse Taparugssanagorn[3], Jari Iinatti[2], and Teemu Myllylä[1,4,5]

[1] Health Science and Technology, Faculty of Medicine, University of Oulu, Oulu, Finland
mariella.sarestoniemi@oulu.fi
[2] Centre for Wireless Communications, University of Oulu, Oulu, Finland
[3] Department of ICT, School of Engineering and Technology, Asian Institute of Technology, Klong Luang, Phatum Thani, Thailand
[4] Optoelectronics and Measurements, Faculty of Information Technology and Electrical Engineering, University of Oulu, Oulu, Finland
[5] Medical Research Center, Oulu, Finland

Abstract. Early cancer detection is crucial, especially for intestinal cancer with subtle early symptoms. While camera-based Wireless Capsule Endoscopy (WCE) systems are efficient, patient-friendly, and safe investigating gastrointestinal (GI) track thoroughly, some limitations persist in visualizing only the inner part of the GI regions. Our study introduces a radio channel analysis -based approach to detect intestinal/abdominal tumors which are not visible for the WCE camera, i.e., the tumors which have started to grow on the outer parts of the intestinal track. Focused on S-parameter patterns in realistic human voxel models, our simulation-based method discerns dielectric property variations in normal and tumorous tissues, replicating intricate tissue characteristics. Preliminary simulation results in different intestine locations demonstrate our technique's efficacy in differentiating normal and tumor cases based on S-parameter patterns. With a 98% accuracy rate, simple logistic regression classification model excels in distinguishing normal from tumor tissues, significantly enhancing diagnostic precision in GI health monitoring showcasing its potential to revolutionize early cancer detection and advance diagnostic accuracy within simulated human anatomy. This represents a substantial stride toward improving healthcare outcomes through cutting-edge technology.

Keywords: Early detection of tumors · Gastrointestinal monitoring · implant communications · ultra-wideband

1 Introduction

Gastrointestinal (GI) tumors encompass a diverse spectrum of lesions, ranging from benign polyps to aggressive malignancies which may represent a significant health burden globally especially in developed countries [1, 2]. Colorectal cancer ranks as the

M. Särestöniemi et al. (Eds.): NCDHWS 2024, CCIS 2084, pp. 426–440, 2024.
https://doi.org/10.1007/978-3-031-59091-7_28

most prevalent gastrointestinal (GI) malignancy [2] whereas small intestine cancer is rare even though small intestine forms a major part of the digestive tract [3]. Small bowl cancers, often originating in inner lining, can extend through various layers [3].

The early detection of intestinal tumors stands as a critical challenge in modern oncology, as timely intervention significantly improves patient outcomes and survival rates [2]. Traditional diagnostic modalities such as computed tomography (CT) [4], magnetic resonance imaging (MRI) [5], and conventional endoscopy with the flexible tube [6] are effective, although often pose limitations in terms of invasiveness, patient discomfort, efficiency, and potential side-effects [6].

Wireless capsule endoscopy (WCE) is attracting attention due to its simplicity and ability to comprehensively examine the gastrointestinal (GI) tract, especially the small intestine, which poses challenges for conventional endoscopy [7]. Persistent challenges include issues such as frame rate, battery life, and automated anomaly detection. Artificial intelligence (AI) assists in image recognition during GI endoscopy, enhancing screening quality and reducing unnecessary costs [8]. Convolutional neural network (CNN) based systems are employed for cancer detection, adding value to colonoscopy based colorectal screening [8].

One main challenge both with conventional endoscopy and capsule endoscopy is that tumors deeply infiltrating the intestinal wall or invading surrounding structures may not be detected since camera's field of view is limited to the mucosal surface of the gastrointestinal tract. Hence, deeper lesions may be beyond its reach. This paper proposes a novel idea of analyzing microwave radio channel between the capsule and on-body antennas which could also reveal tumors which are not visible for capsule camera.

In this paper, we propose WCE radio channel analysis-based detection of tumors which are not visible for capsule endoscopy cameras. The radio channel analysis could be used as an additional feature to the traditional WCE. To the best of our knowledge, none of the previous studies have explored the detectability of tumors, which are outside the visibility of the capsule endoscopy camera, using radio channel-based analysis. Our methodology revolves around radio signal recognition, specifically analyzing channel transfer parameters S_{N1} between the capsule and the on-body antennas, with N being the number of on-body antennas. In contrast to conventional visual-based methods, our simulation-centric approach utilizes S_{N1} patterns to discern variations in dielectric properties, such as relative permittivity and conductivity, between normal and tumorous tissues. By leveraging realistic human voxel models, our approach aims to faithfully replicate intricate tissue characteristics, providing a nuanced understanding of the subtle differences that indicate the presence of tumors.

Our initial simulation findings, conducted with a realistic voxel model, underscore the effectiveness of our method in distinguishing between normal and tumor cases based on SN1 patterns. By utilizing SN1 pattern analysis, we not only enhance precision in the WCE system but also highlight its potential to redefine strategies for early cancer detection of the tumors non-visible for capsule cameras. This advancement contributes to improved diagnostic accuracy within a simulated realistic human anatomy, paving the way for transformative developments in the field.

Our study focuses on automatically distinguishing between normal and tumorous tissues in colon and small intestine areas using SN1 patterns. Besides of analyzing differences in SN1 patterns, our further objective is to implement a classification approach by employing Logistic Regression as a straightforward yet effective method. The classification model is trained on a labeled dataset, where SN1 patterns serve as features, and corresponding labels indicate tissue status (0 for normal, 1 for tumorous). Through this approach, we aim to achieve automated discrimination, thereby advancing early cancer detection strategies.

The paper is structured as follows: Sect. 2 provides description of simulation models, dielectric properties of tumor and normal tissues, as well as details about antennas and their locations. Additionally, evaluated capsule and tumor locations are illustrated in the small intestine and colon regions. Section 3 presents the radio channel evaluations in the presence and absence of tumors in small intestine and colon areas. Section 4 presents Logistic Regression Classification results. The paper concludes with a summary and outlines the potential future works in Sect. 5.

2 Methodology

2.1 Simulation Models

The investigation employs computer systems technology (CST), an electromagnetic simulation software utilizing the finite integration technique [9]. An anatomical voxel model is utilized, and WCE-model, equipped with a dipole antenna, is strategically positioned within various segments of the small intestine in the voxel model. To establish an in-to-out wireless body area network (WBAN), a highly directive on-body antenna is integrated. Notably, the radio channel characteristics undergo significant variations depending on the placement of the on-body antenna within the intestines and its proximity to the WCE-model. Therefore, careful selection of on-body antenna locations becomes essential to ensure comprehensive coverage across the entire intestinal area.

It is important to highlight that path loss emerges as a primary constraint in the investigation. This constraint is influenced by both the distance between the capsule and the on-body antenna, and the tissues situated between them. Hence, a nuanced consideration of path loss, incorporating both distance and tissue characteristics, is crucial for the successful execution and interpretation of the investigation.

Among the voxel models provided by CST, the anatomical voxel model named Laura, depicting a middle-aged female body with a resolution of $1.87 \times 1.87 \times 1.25$ mm, is chosen due to its accurate modeling of the intestinal region including subcutaneous and visceral fat, muscles, small intestine (wall and content), and colon (large intestine). Table 1 furnishes the dielectric properties of various human body tissues at 4 GHz [10] including dielectric tumors of intestinal tumor retrieved from [11]. Table 1 also includes tissue thicknesses in capsule location A.

2.2 Antennas and Antenna Locations

In conventional WCE, the integrated camera captures images while navigating the GI tract, transmitting them to a monitoring device on the user's belt. The patient returns the

Table 1. Voxel model thickness at the selected crosscut and tissues' dielectric properties at 4 GHz.

Tissues	Thickness [mm]	Permittivity [F/m]	Conductivity [S/m]
Skin	1.4	36.6	2.34
Fat (subcutaneous)	15	5.31	0.18
Muscle	9	50.8	3.01
Fat (visceral)	4	5.31	0.18
Small intestine (wall)	8	50.8	3.11
Small intestine (content)	20	51.7	4.62
Intestinal tumor [11]	1 cm/2 cm/3 cm	57	5.2

monitoring device to the doctor the following day for image review. Nevertheless, the potential for doctors to remotely monitor real-time images presents a valuable opportunity. Our proposed idea facilitates comprehensive GI track and surrounding area monitoring through radio signal transmission. The integration of an in-to-out WBAN, 5G functionalities and a straightforward classification approach makes real-time tumor detection achievable [12, 13]. The IEEE802.15.6 standard for WBAN defines the frequency range in Ultra-Wide Band (UWB), specifically 3.1–10.6 GHz [14]. Considering propagation losses, our study utilizes the lower segment of the UWB band for capsule endoscopy (3.75–4.25 GHz).

In our research, on-body antennas are designed for 3.75–4.25 GHz, meeting IEEE802.15.6 standard requirements and falling within the 5G frequency range 3.3–4.2 GHz) used in the USA and partly in Europe. A cavity-backed low-band UWB directive antenna type (Fig. 1a) is chosen for on-body antennas due to its good directivity, aligned with IEEE 802.15.6 standard requirements [14]. Details of the antenna characteristics and its radiation patterns are presented in [15]. Five on-body antennas are used to cover small and large intestinal areas thoroughly as shown in Fig. 1b. The antennas are numbered according to their port number in the simulation model (port number 1 for the capsule antenna, port numbers 2–6 for on-body antennas), as described in our WCE channel modeling paper in [16, 17].

As a capsule model, we used a small dipole embedded inside a realistic shaped and sized capsule shell, as described in [16]. The evaluated capsule and tumor locations are presented in Fig. 2a-b in small intestine and in Fig. 2c-h in large intestine areas. Location in small intestine is named as MI00, similarly to our previous study presenting radio channel modeling with realistic models [17]. Locations in large intestines are named as "Loc. D" (Fig. 2c-d), "Loc. C" (Fig. 2e-f), and "Loc. A" (Fig. 2g-h), also similarly to [13]. These capsule locations are chosen to present different propagation conditions in abdominal area between the capsule and the on-body antenna - in terms of different thicknesses of fat and muscle tissues as well as capsule location respect to the closest on-body antennas.

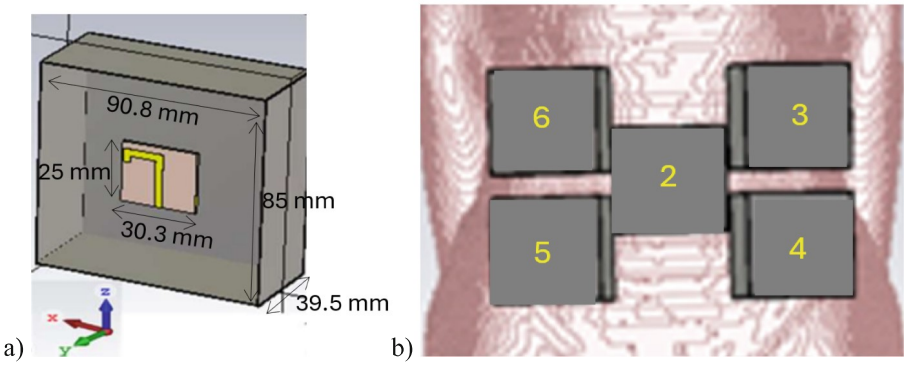

Fig. 1. a) The cavity-backed low-band UWB directive on-body antenna designed for in-body communications, b) locations of five on-body antennas [16].

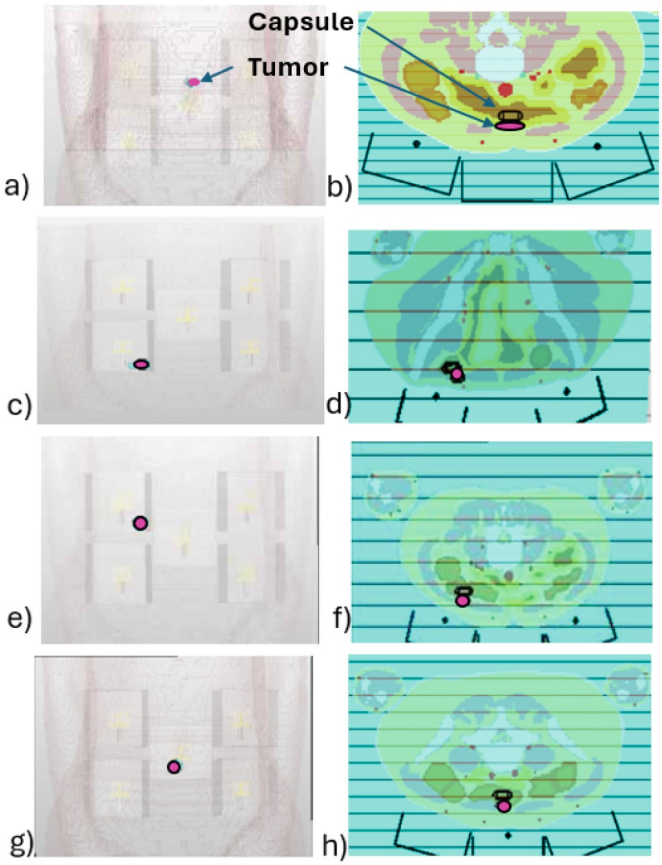

Fig. 2. The locations of tumors and capsule respect the on-body antennas and corresponding cross-section illustration a-b) Loc. MI00 (small intestine), c-d) Loc. D (colon), e-f) Loc. C (colon) and g-h) Loc. A (colon).

3 Results: Impact of the Tumors on Channel Characteristics

In this section, the channel characteristics between the capsule model and the on-body antennas are evaluated in several locations of Laura-voxel's intestine. Due to brevity, the focus is showing the S-parameters in the presence and absence of tumors especially in the colon area, where most of the GI tumors usually grow. Additionally, an example case for small intestine area is also presented to demonstrate the efficiency of the method.

3.1 Impact of the Tumor in Small Intestinal Area

Firstly, radio channel characteristics are evaluated in small intestinal tumor case, in location MI00. In this case, three tumor sizes are evaluated: with the widths 1 cm (small), 2 cm (medium), and 3 cm (large). All of them are located inside the small intestine wall without visibility to the interior of the small intestine where WCE moves.

The channel parameters between the capsule and on-body antenna S_{21}, S_{31}, S_{41}, S_{51} and S_{61} are presented in Fig. 3a-e. As can be seen, the impact of the tumors is visible in all the simulated channel parameters even with the smallest tumor. The impact of the tumor varies significantly with the frequency. The changes due to small tumor vary from 0.01–4 dB whereas due to the large tumor 0.1–25 dB.

3.2 Impact of Tumors on Channel Characteristics in Colon Area

Location D

Next, the evaluations are carried out in different locations of the colon area, first in Loc. D illustrated in Fig. 4a-b. This centralized location is demonstrated first to show how tumors which are non-visible for the capsule camera, may change channel characteristics between the capsule and all the surrounding antennas. The results for S_{21}, S_{31}, and S_{41} parameters are shown in Fig. 6a and for S_{51} and S_{61} in Fig. 6b. It is found that tumor located on the outer surface of the colon, causes clear differences in S-parameters. The smallest differences are found in the channel response, which is closest to the capsule, in this case S_{21} parameter: maximum difference is 5 dB at 5 GHz, but within the antenna's specific operational frequency range 3.75–4.25 GHz, the maximum difference is only 1 dB. Instead with S_{61}, the maximum difference within the antenna's operational range is even 7 dB. This phenomenon is due to the capsule's location exactly in the same horizontal line as the radiator of the on-body antenna 2 as well as due to the large size on the on-body antenna which captures multipath signal components from large area around the capsule. Hence the tumor which is located exactly on the front of the capsule in this scenario, does not affect significantly. However, it is assumed that with a smaller cavity, or with the same antenna without the cavity, the impact would be more significant.

Location C

Next, the channel characteristics are evaluated in Location C which is on the down right corner of the on-body antenna 6's cavity. In this case, we evaluated the impact of the tumor of two sizes 1 cm (small) and 3 cm (large). The results are presented in Fig. 5a-e. Also in this case, the tumor has an impact on the channel characteristics of all the on-body antennas. Now even the impact is larger than in the on-body antenna location D

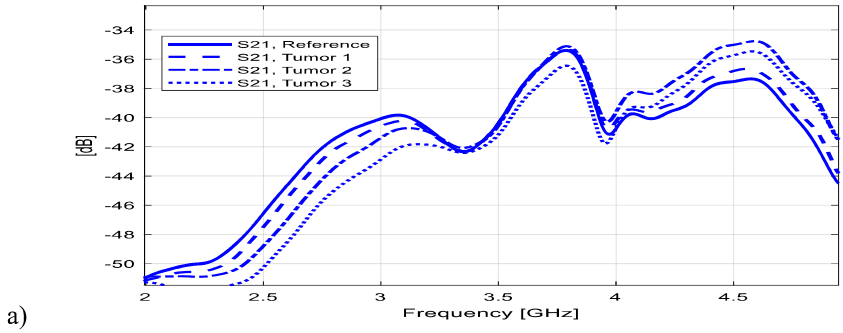

a)

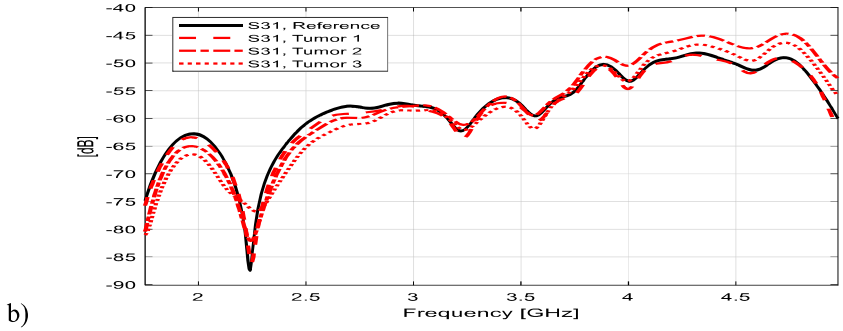

b)

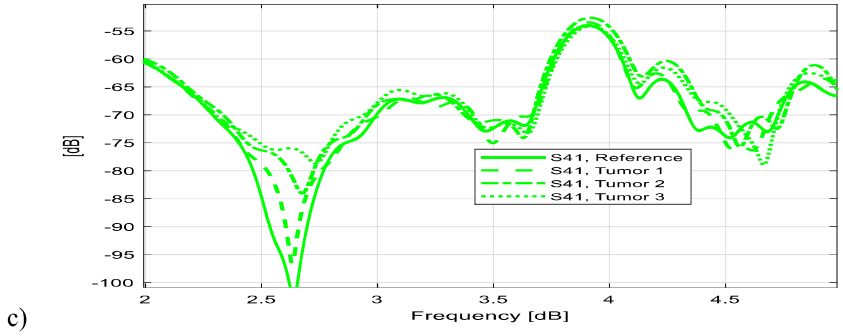

c)

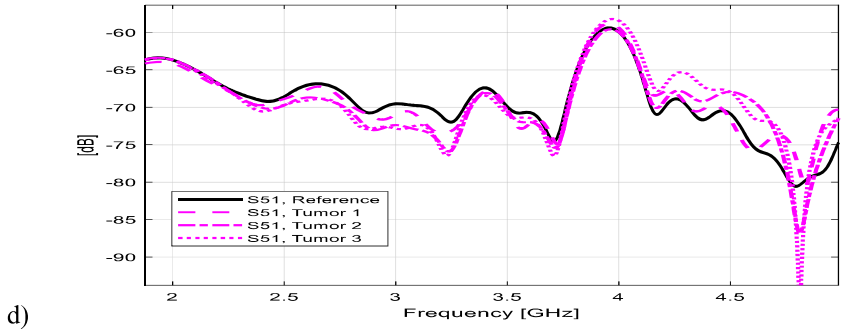

d)

Fig. 3. Channel characteristics between the capsule and the on-body antennas in the small intestine region in the presence of tumors having sizes 1cm, 2 cm and 3cm: a) S_{21}, b) S_{31}, c) S_{41}, d) S_{51}, e) S_{61} results.

e)

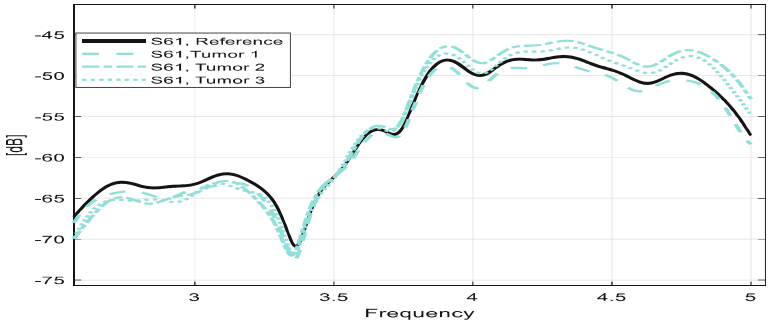

Fig. 3. (*continued*)

since the capsule is not located in the middle of the antenna's cavity. The larger tumor has naturally larger impact on the channel characteristics. The maximum difference between the larger tumor and reference case is over 20 dB whereas with smaller tumor the maximum difference is few decibels.

Location A

Finally, an assessment of the channel characteristics is conducted at Location A, and the results are illustrated in Fig. 6a-c. This analysis includes the examination of capsule antenna reflection coefficients S_{11}, a commonly utilized parameter in tumor detection. The findings reveal that, in this specific case of tumor and capsule placement, tumors induce only negligible changes in the S_{11} parameters. Consequently, it is determined that S_{11} is not conducive to effective tumor detection under these circumstances. Instead, variation with channel parameters is obvious and clearly detectable: the difference is even over 20 dB in several frequencies.

It is crucial to note that manually or visually inspecting a substantial amount of data for such differences is impractical. Therefore, in the pursuit of a more systematic approach, the next subsection introduces automatic classification modeling. This approach allows for a comprehensive analysis and categorization of the data, ensuring efficient identification of patterns indicative of normal and tumor tissue conditions.

4 Logistic Regression Classification Results

Logistic regression emerges as a robust statistical model tailored for binary classification challenges, precisely aligning with our objective of distinguishing between normal tissue and tumor tissue. Comprising key components, the logistic regression model incorporates extracted features from the S_{21} as input features ($\boldsymbol{X}$), encapsulating vital channel response characteristics. The output variable ($\boldsymbol{Y}$) denotes the binary class assignment (normal or tumor). Employing the sigmoid activation function $\boldsymbol{\sigma}(z) = \frac{1}{1+\mathbf{exp}(-z)}$, the model transforms the linear combination of input features into probabilities, ensuring outputs fall within the 0 to 1 range, signifying the likelihood of belonging to the positive class (tumor) [18–20]. The linear combination, expressed as the logit function [20]

$$\hat{p} = \beta_0 + \beta_1 X_1 + \beta_2 X_2 + \ldots + \beta_n X_n, \tag{1}$$

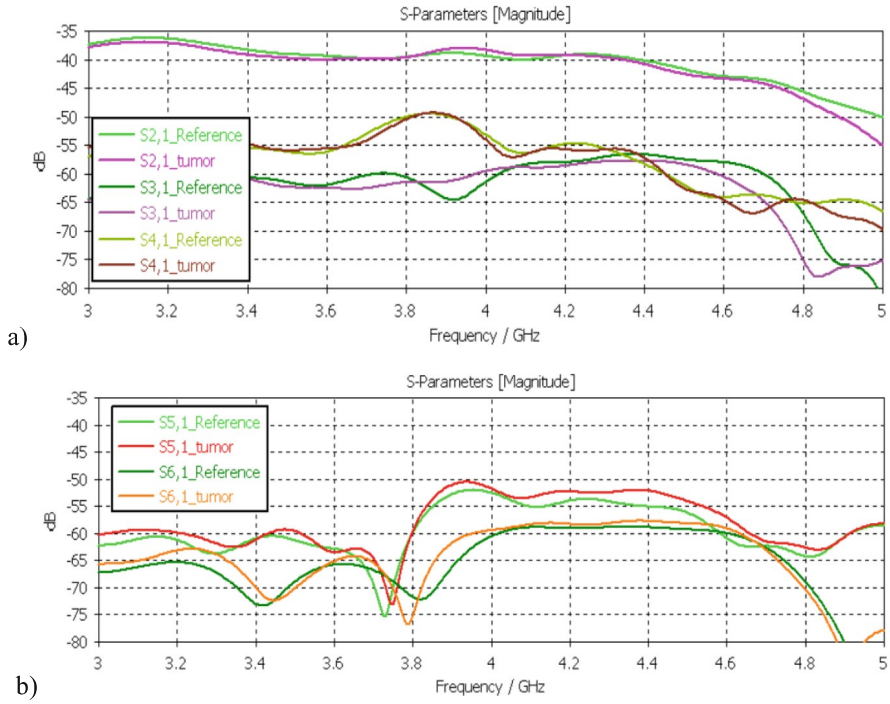

Fig. 4. S_{21}-S_{61} parameters in the presence and absence of small and large tumors and reference case in capsule and tumor locations D in colon.

computes the log-odds, with coefficients ($\boldsymbol{\beta}$) associated with input features determining the probability of the positive class.

In the training phase of logistic regression, the model learns from a labeled dataset to optimize its coefficients (β) for accurate predictions. The objective is to find the values of β that minimize the difference between the predicted probabilities and the actual class labels. This process is often achieved through optimization techniques, with two common methods being Maximum Likelihood Estimation (MLE) and gradient descent.

Maximum Likelihood Estimation (MLE): This statistical method aims to maximize the likelihood function, which measures the probability of observing the given dataset under the assumed statistical model. In logistic regression, MLE finds the set of coefficients (β) that maximizes the likelihood of observing the actual outcomes given the input features [20].

Gradient Descent: An iterative optimization algorithm, gradient descent adjusts the coefficients (β) by moving towards the minimum of the cost function. The cost function quantifies the difference between predicted probabilities and actual labels. By calculating the gradient of the cost function with respect to the coefficients, the algorithm updates β in the direction that minimizes the cost, gradually converging towards the optimal values [20].

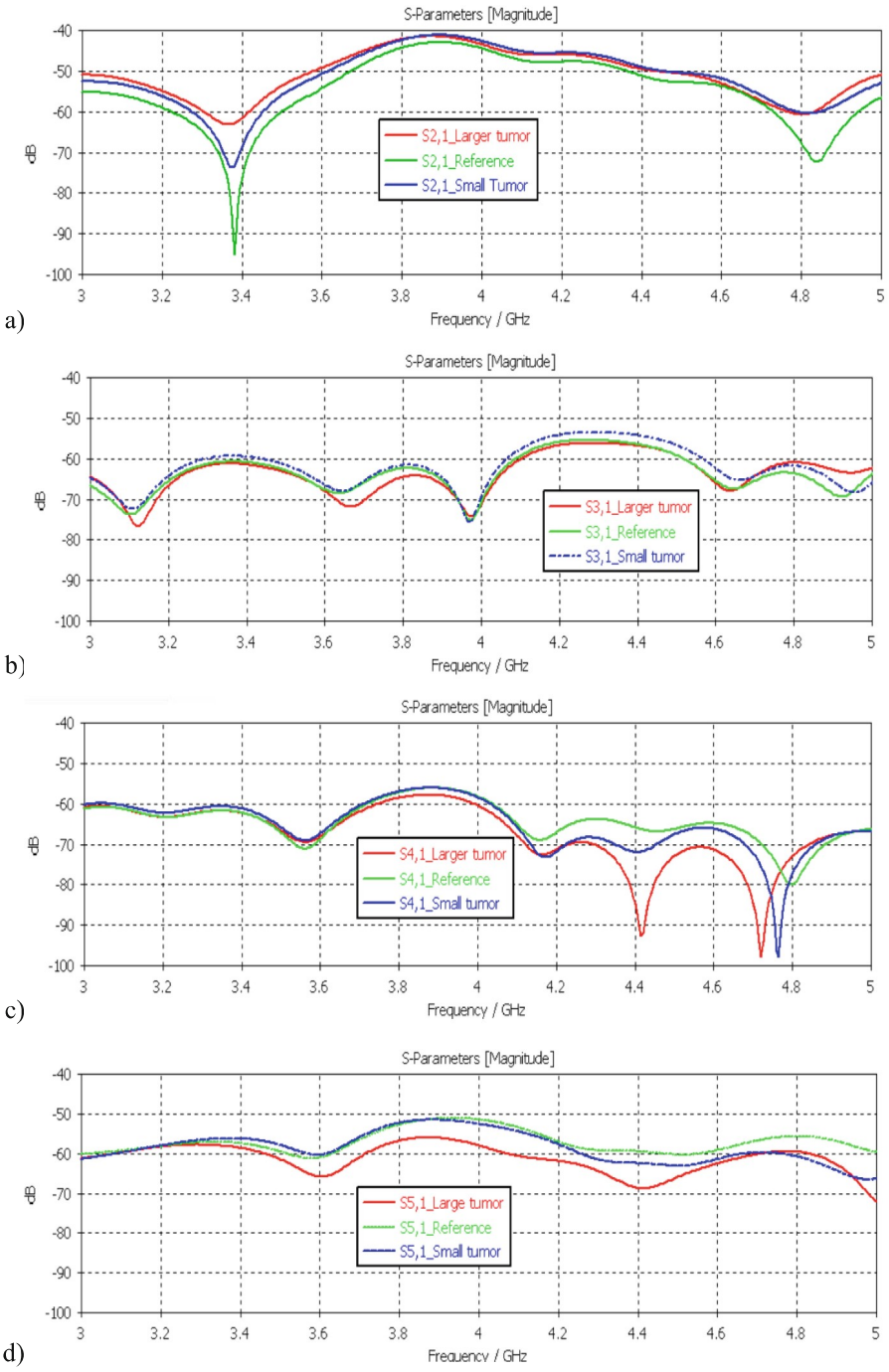

Fig. 5. S_{21}-S_{61} parameters in the presence and absence of small and large tumors and reference case in capsule and tumor locations C.

e)

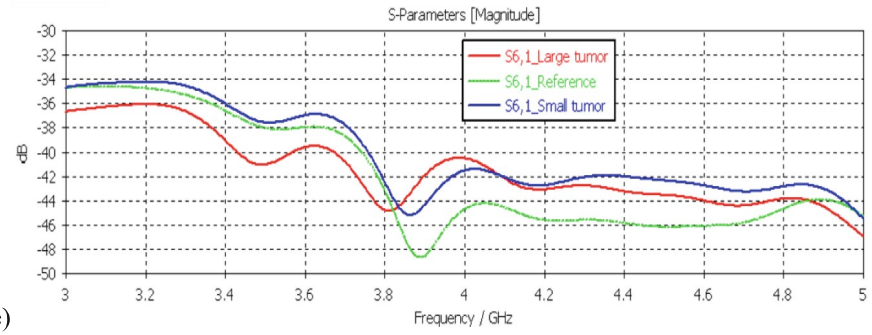

Fig. 5. (*continued*)

Both MLE and gradient descent play crucial roles in refining the logistic regression model during training, ensuring it captures the underlying patterns in the data and can make accurate predictions on new, unseen examples. This iterative process of adjusting coefficients enhances the model's ability to discern between normal and tumor tissue cases based on the extracted features from S_{21}.Evaluation metrics, including accuracy, precision, recall, and F1-score, play a crucial role in assessing the proficiency of the logistic regression model in classifying normal and tumor cases. Accuracy, represented by [10].

$$Accuracy = (TP + TN)/(TP + TN + FP + FN), \tag{2}$$

gauges the overall correctness of the model's predictions, considering true positives (TP), true negatives (TN), false positives (FP), and false negatives (FN). Precision expressed as [20].

$$Precision = TP/(TP + FP), \tag{3}$$

evaluates the model's ability to correctly identify positive cases among all predicted positives. Recall, denoted by [20].

$$Recall = TP/(TP + FN), \tag{4}$$

$$F1score = (2Precision\,Recall)/(Precision + Recall), \tag{5}$$

provides a balanced assessment, considering both false positives and false negatives. These metrics collectively offer a comprehensive evaluation of the logistic regression model's performance, highlighting its strengths in binary classification tasks. In summary, logistic regression emerges as a powerful and reliable solution for intestinal tumor detection, even those outside the visibility of WCE camera, excelling in simplicity, interpretability, and efficacy.

Building upon the foundations laid in the preceding sections, our investigation into Channel Frequency Response (CFR) using the S_{N1} parameter revealed compelling insights. In the CFR analysis, distinctive patterns emerged between normal and tumor

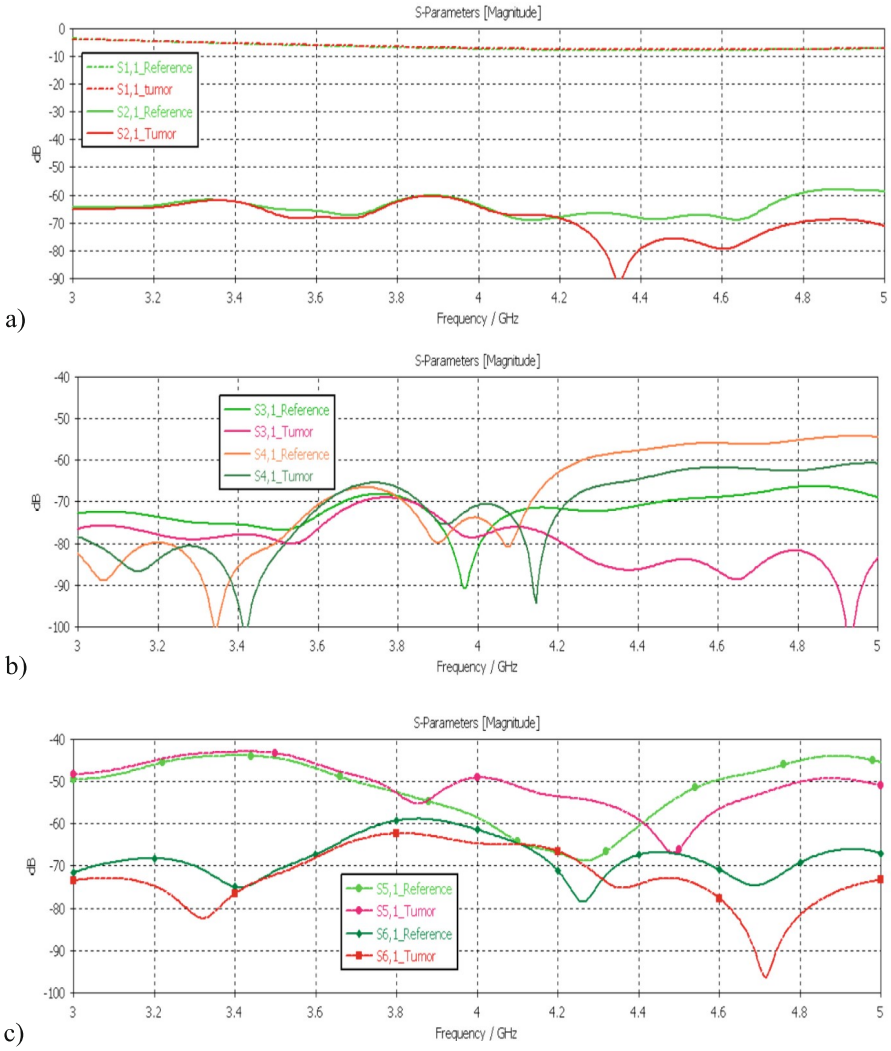

Fig. 6. a) S_{11} and S_{21} parameters, b) S_{31}, S_{41} parameters and c) S_{51} and S_{61} parameters in the presence and absence of tumors in capsule and tumor location A.

cases, affirming the capability of wireless capsule endoscopy data to capture nuanced differences in electromagnetic interactions within the small intestine. These findings set the stage for a detailed examination of the results derived from logistic regression modeling.

The application of logistic regression for intestinal tumor detection showcased excellent outcomes, achieving a remarkable accuracy of 98% with this initial data set consisting of 20 samples. The precision of the model, indicating its ability to correctly identify tumor cases among the positive predictions, stood at an outstanding 96%. Recall, reflecting the model's capacity to capture all actual tumor cases, demonstrated an impressive

rate of 97%. Additionally, the F1-score, a balanced metric considering both precision and recall, reached an excellent level of 96%. Trained on labeled datasets, the model not only displayed commendable performance across multiple metrics but also provided interpretability, enhancing our understanding of the impact of extracted features on classification decisions. Logistic regression emerged as a practical tool for our proposed methodology.

The results obtained with this initial data set, highlighted by an outstanding 98% accuracy, coupled with impressive precision (96%), recall (97%), and F1-score (96%), validate the robustness of our methodology. In addition to effectively distinguishing between normal and tumor tissues, these outcomes hold promise for advancing diagnostic accuracy in GI health monitoring. The interpretability and computational efficiency of logistic regression significantly contribute to the practicality of our approach. Future research endeavors may focus on refining the model, incorporating additional features, and expanding the dataset to enhance its clinical applicability. In essence, our findings represent a substantial advancement in the evolution of wireless capsule endoscope localization and small intestinal polyp detection.

5 Conclusions and Future Works

This study introduces a groundbreaking approach to detecting non-visible intestinal using WCE with radio channel analysis feature. Through the integration of CFR analysis and logistic regression modeling, the study achieves remarkable results. The presence of tumors effects clearly on the channel characteristics between the capsule and the closest on-body antennas although the tumors are not visible for WCE. The logistic regression model carried out to initial data set exhibits an impressive accuracy of 98%, demonstrating outstanding precision, recall, and F1-score in distinguishing between normal and tumor tissues. This achievement holds great promise for advancing diagnostic accuracy in gastrointestinal health monitoring even for the cases where tumors are not visible for capsule camera.

As a future work, we will evaluate a more comprehensive study with different tumor types, different tumor locations, as well as using voxel models having different body constitutions. Additionally, exploration of deep learning models, capitalizing on their ability to discern intricate patterns within more extensive datasets. Models like CNN or Recurrent Neural Networks (RNNs) could elevate the sophistication of our current model, potentially enhancing its performance across diverse and expansive datasets. Moreover, ongoing refinement and expansion of the dataset could significantly bolster the model's robustness. The inclusion of additional features, such as patient-specific information or real-time physiological data, has the potential to provide a more comprehensive context for improved classifications. Collaborative efforts with medical professionals to validate the model's outcomes in clinical settings would further establish its practical applicability. In essence, the success achieved in this study lays a solid foundation for future advancements in WCE localization and intestinal tumor detection. The integration of cutting-edge technologies, particularly deep learning, holds the promise of pushing the boundaries of accuracy and reliability in GI monitoring.

Acknowledgments. This research is funded by Academy of Finland Profi6 funding, 6G-Enabling Sustainable Society (University of Oulu, Finland).

Disclosure of Interests. The authors have no competing interests to declare that are relevant to the content of this article.

References

1. Stewart, W.B.W., Christopher, P.: World cancer report from world health organization (WHO) (2014)
2. Jardim, S.R., de Souza, L.M.P., de Souza, H.S.P.: The rise of gastrointestinal cancers as a global phenomenon: unhealthy behavior or progress? Int. J. Environ. Res. Public Health **20**(4), 3640 (2023). https://doi.org/10.3390/ijerph20043640
3. Chamberlain, R.S., Krishnaraj, M., Shah, S.A.: Chapter 54: cancer of the small bowel. In: DeVita, V.T., Lawrence, T.S., Rosenberg, S.A. (eds.) DeVita, Hellman, and Rosenberg's Cancer: Principles and Practice of Oncology. 10th ed. Lippincott Williams & Wilkins, Philadelphia (2015)
4. Aaron, F.: The history, development and impact of computed imaging in Neurological Diagnosis and Neurosurgery: CT, MRI, and DTI. Nat. Proc. **1**(1), 76 (2009)
5. Haacke, E.M., Brown, R.F., Thompson, M., Venkatesan, R.: Magnetic resonance imaging: physical principles and sequence design. Wiley, New York (1999) ISBN 978–0–471–35128–3
6. Yuce, M.R., Dissanayake, T.: Easy-to-swallow wireless telemetry. IEEE Microwave Mag. **13**(6), 90–101 (2012)
7. Ciuti, G., Menciassi, A., Dario, P.: Capsule endoscopy: from current achievements to open challenges. IEEE Rev. Biomed. Eng. **4**, 59–72 (2011)
8. Gao, H., Lin, S., Yang, Y., Li, C., Yang, M.: Convolution neural network based on two-dimensional spectrum for hyperspectral image classification. J. Sens. **2018**, 13 (2018)
9. CST Microwave Studio. http://www.cst.com
10. https://www.itis.ethz.ch/virtual-population/tissue-properties/database
11. Guardiola, M., et al.: Dielectric properties of colon polyps, cancer, and normal mucosa: ex vivo measurements from 0.5 to 20 GHz. Med. Phys. **45**(8), 3768–3782 (2018)
12. Teshome, A.K., Kibret, B., Lai, D.T.H.: A review of implant communication technology in WBAN: progress and challenges. IEEE Rev. Biomed. Eng. **12**, 88–99 (2019). https://doi.org/10.1109/RBME.2018.2848228
13. Leelatien, P., Ito, K., Saito, K., Sharma, M., Alomainy, A.: Channel characteristics and wireless telemetry performance of transplanted organ monitoring system using ultrawideband communication. IEEE J. Electromagnet. RF Microwaves Med. Biol. **2**(2), 94–101 (2018). https://doi.org/10.1109/JERM.2018.2827779
14. IEEE Standard for Local and metropolitan area networks Part 15.6: Wireless Body Are Networks, pp. 1–271. IEEE (2012)
15. Kissi, C., Särestöniemi, M., Pomalaza-Raez, C., Sonkki, M., Srifi, M.N.: Low-UWB directive antenna for wireless capsule endoscopy localization. In: Proceedings of the 13th EAI International Conference on Body Area Networks (2018)
16. Särestöniemi, M., Pomalaza-Raez, C., Kissi, C., Berg, M., Hämäläinen, M., Iinatti, J.: WBAN channel characteristics between capsule endoscope and receiving directive UWB on-body antennas. IEEE Access Spec. Sect. Body Area Netw. **8**, 55953–55968 (2020)

17. Särestöniemi, M., Taparugssanagorn, A., Wisanmongkol, J., Hämäläinen, M., Iinatti, J.: Comprehensive analysis of wireless capsule endoscopy radio channel characteristics using anatomically realistic gastrointestinal simulation model. IEEE Access **11**, 35649–35669 (2023). https://doi.org/10.1109/ACCESS.2023.3263555
18. Eren, L.: Bearing fault detection by one-dimensional convolutional neural networks. Math. Probl. Eng. **2017**, 1–9 (2017). https://doi.org/10.1155/2017/8617315
19. Venna, S.R., Tavanaei, A., Gottumukkala, R.N., Raghavan, V.V., Maida, A.S., Nichols, S.: A novel data-driven model for real-time influenza forecasting. IEEE Access **7**, 7691–7701 (2018)
20. Hosmer, D.W., Lemeshow, S., Sturdivant, R.X.: Applied Logistic Regression. Wiley (2013)